DIALOGUE SOCIAL SCIENCE REVIEW

Manipulation of Spectral Hole Burning in Atomic Medium by Doppler Broadening Effect

Zahid Noor
Department of Physics University of Peshawar.
Email: zahidkhan3212020@gmail.com

Samiur Rahman
Department of Physics University of Malakand. Email: samiurhman12@gmail.com

Najeeb Ullah
Department of Physics University of Malakand. Email: nk190945@gmail.com

Muhammad Umair
Department of Physics University of Peshawar.
Email: muhammadumairpk77@gmail.com

Abstract
Spectral holes burning are controlled and modified in a four-level sodium hot atomic medium. Two spectral holes are measured in the absorption spectrum, which are associated with steep normal dispersive regions. The group velocity is slowed down in this normal dispersive region from vacuum speed vg << c. The spectral hole occurs at the phase pc — T/ 2 with equal depths and equal normal dispersion on both sides of the resonance point. The spectral hole occurs at the phase pc < T/ 2 with unequal depths and unequal normal dispersion on both sides of the resonance point. The depth of the spectral hole at the negative detuning is smaller, and the spectral hole at positive detuning is larger when pc < n/ 2, while it shows contrasting behavior at pc > T/ 2. This work shows significant variation in spectral holes with the collective phase of control fields and the corresponding enhanced and degraded steepness of normal dispersion in the regions of spectral holes burning.

key word: Spectral Hole Burning, Four-Level Atomic System, Group Velocity Modulation, Normal Dispersion Control.

Introduction
Optical hole burning is a phenomenon in which a saturating field creates a "hole" in the population distribution of an inhomogeneous medium. This process is extensively applied in atomic, molecular, and solid-state physics, offering promising advancements in areas such as data storage (optical memory) and signal processing. It is also utilized for applications like frequency stabilization, optical tomography, photosynthesis, and spectral-spatial correlations. The concept was first demonstrated by Schwartz and Tan, who observed spectral hole burning in the absorption spectrum using density matrix formalism. They discovered that even with homogeneous broadening mechanisms, a strong wave

could produce absorption holes when probed with another wave. Persistent spectral holes were later identified in solid impurities at low temperatures, further expanding its potential applications. Researchers such as Shakhmuratov and Szabo explored the impact of phase noise on coherent hole burning, while others, including Dong and Gao, observed this phenomenon in ladder-type atomic configurations with coupling and saturating lasers. Comparisons of ladder-type, V-type, and A-type atomic configurations revealed that spectral hole burning is particularly significant in A-type systems. The Doppler broadening effect, which is temperature-dependent, plays a crucial role in shaping the dynamics of spectral hole burning. This effect occurs due to the relative motion of particles along the propagation path of light, causing broadening of spectral lines. Researchers have investigated light pulse propagation in Doppler-broadened media, emphasizing its implications for hole burning. Recent studies have demonstrated how controllable hole burning can be achieved within Doppler absorption profiles by employing saturating and coupling fields. Advances in this field have also enabled the reduction of light pulse speed in the hole-burning region, with rubidium vapors being a notable example. Spectral hole burning in a four-level sodium atomic medium demonstrates how coherent driving fields influence the phenomenon under Doppler broadening. Applications of this effect, such as optical tomography and photosynthesis, highlight its significance in both scientific research and practical implementations.

Literature Review

Spectral hole burning (SHB) occurs when carriers at specific energy levels cannot replenish vacancies caused by strong stimulated recombination at those levels. This results in holes within the energy band, often twice the width of the homogeneous linewidth, provided the laser linewidth is significantly narrower. However, this method can be challenging to implement due to stringent requirements for laser frequency and power stability. Additionally, excessive laser intensity can lead to broadening of the spectral hole, complicating the process.

In dynamic SHB, a hole forms on one side of the spectrum and gradually recovers over time. Molecules of dimensions comparable to the wavelength of incident light often do not interact with the light, exhibiting distinct absorption properties. The behavior of dynamic SHB is influenced by the intensity of light waves, which determines the extent of the spectral hole formation.

Persistent SHB results in a permanent hole in the absorption spectrum following the excitation of particles in the medium. Persistent SHB often leads to irreversible changes, such as molecular damage or permanent bleaching in an inhomogeneous absorption spectrum. Persistent SHB is also observed in materials like CdSe and CuCl nanocrystals. Applications of persistent SHB include optical signal processing, optical data storage, and pulse shaping.

Several factors impact the occurrence and characteristics of SHB in a material, including: Intensity of the absorbed light, Duration of the absorption process, Material temperature

SHB is a notable effect of mode competition, where multiple optical modes vie for energy levels in laser systems. This competition significantly reduces amplifier gain across competing frequency bands, as seen in Doppler-broadened

emissions. The laser's output spectrum density is influenced by the Doppler-broadened beam width.

SHB plays a vital role in quantum optics, offering a pathway for spectroscopy in solid materials. It enables differentiation of hyperfine level transitions and finds use in diverse applications such as photosynthesis, optical tomography, temporal cloaking, memory storage, and information retrieval. Additionally, SHB facilitates laser frequency stabilization by producing a narrow spectral hole in the absorption profile.

Electric susceptibility refers to a material's ability to polarize in response to an applied electric field. Represented as a dimensionless proportionality constant, susceptibility measures the relationship between polarization and the applied field. As the electric field increases, polarization also increases proportionally, and vice versa. Typically, polarization in a dielectric is directly proportional to the applied electric field. However, an increase in the external electric field reduces the total electric field within the material. Mathematically, polarization P is related to the electric field E as:

$$P = \epsilon_o E + P$$
$$D = \epsilon_o (1 + \chi_e) E$$
$$D = \epsilon_r \epsilon_o E$$

Doppler broadening refers to the widening of spectral lines due to velocity distributions of atoms or molecules, resulting in Doppler shifts. These shifts collectively cause broadening of emission or absorption lines, producing a characteristic Doppler profile. A notable case is thermal Doppler broadening, where the effect arises from the thermal motion of particles. The broadening depends on the spectral line frequency, particle mass, and temperature, making it a useful tool for deducing the temperature of emitting or absorbing bodies under spectroscopic investigation.

Doppler broadening increases proportionally with the square of temperature, inversely with the square of particle mass, and directly with source frequency. It provides critical insights into the dynamic properties of emitting or absorbing systems.

Method of Calculation
Model of The Atomic System

Our proposed N-type cesium atomic model is shown in Fig. 1. In this system a probe field of rabi frequency Gp is coupled between levels 1) and 4). Control fields of rabi frequencies Gl G} 2) Gl Gl $21e-i(01^{,\theta_2})$ are also applied in the system. The detunings of these fields are denoted as A 3 respectively. The decay rates from the excited to the ground levels are expressed as$\gamma_{41,42,43,3}$ To explain the equations of motion and optical properties of the system, we proceed with the following interaction picture Hamiltonian in the dipole and rotating wave approximations:

$$= -\frac{}{2} [\, Gpe \qquad 1)\,(41 - iA1t\ 2)\,(4$$
$$+ G_2 e - iA2t\ 3)\,(41 + G3e^{-}tA3t\ 2)\,(31] + H.\,c.$$
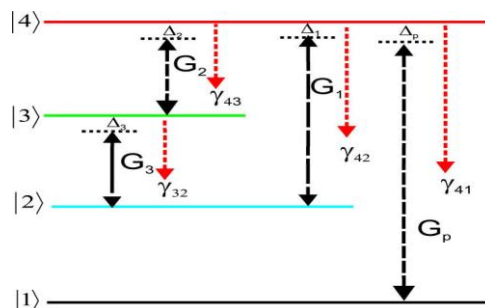
Energy diagram of four level atomic system:
The detunings parameters are related to the angular frequencies of these fields and atomic states resonant frequencies such as: Al = —WI, A2 = —w2, A3 L'23 — and A (DI4 — cop, where WI4, L'23, L'24 and are the resonant frequencies between the two states. Here WI, and wp are the frequencies of the control and probe fields respectively. The general form of
density matrix equation is given by the following relation:

$$ \gamma_{ij} \quad \frac{dp}{dt} = ill, \text{- E}(oa^t p + poo^t — 2o^t pa) \text{ (3.2) p] 2} $$

where a^t and a are raising and lowering operators respectively. Eq.(2) is used for the dynamical solution of the proposed system and the following four coupled rates equations are obtained: P14 — [iAp -741]P14 + Gp(P44 — P11) ̄ G 1 PI '2 ̄ G2P13'

$$ _{12} \;=\; [(i\Delta_p - i\Delta_1) - \frac{˜}{ɔ}(\gamma_{41} + 742 + \qquad + GpP42 $$

2

$$ \underline{}^G IP14 — G3P13 $$
$$ 2 \qquad 2 $$
$$ P13 \qquad [(iAp - iA2) - — (741 + 743]P13 + Gp(P43 $$

2

$$ \underline{}G2P14 — $$
$$ 2 \qquad 2 $$

First order perturbation approximations and initial population condition are applied to solve Eqs. (3-6) analytically by the following relation.

$$ Y(t) = \int_{-\infty}^{t} e^{-Z(t-t')} M dt' \qquad = Z^1 M $$

Where Y (t) and M are column matrices while Z is a 3x3 matrix. Expression for   is obtained and written as:
i (4.42±13   Gp
    14 ̄
         2(A3 G} + A2 C;} +   +   + i Gl G2 G3 cos[pc])
where
1
                   Al   i Ap ̄ 0/41
Susceptibility of the optical medium is a complex response function to the

applied electric field. Its real and imaginary parts are associated with the probe dispersion and absorption spectrum respectively. To evaluate susceptibility for this atomic configuration, we define the electric polarization of the medium as p eo XE and due to the probe field coherence polarization is P=Ip141 PI 4. Here PI4 is the dipole matrix element. The complex susceptibility for the system is obtained by comparing the two polarizations:

2NP14~

$$\chi = \overline{\frac{2NP_{14}}{\epsilon_0 \hbar \, G_p}} \rho_{14}$$

To introduce the Doppler effect in the medium, the detuning parameters Ap is replaced by Ap -4- kv and Al is replaced by Al + rnkv, while A2 is replaced by A2 - 4- r)2kv. where and is the propagating direction of the corresponding driving fields. In this replacing of detuning the susceptibility is become velocity dependent and is written as x(kv). The susceptibility of the medium endowed with Doppler character is given by taking the average of x(kv) over the Maxwellian distribution as:

where VD is the Doppler width and depends upon the absolute temperature. Its value is written as: VD ICBTw;/Mc² ² where wp is the frequency of probe field, KB is the Boltzman constant, T is the absolute temperature, M is the molecular mass and c is the speed of light in vacuum.

$$\chi_D = \frac{1}{V_D \sqrt{\pi}} \int_{-\infty}^{\infty} e^{-\frac{(kv)^2}{V_D^2}} \chi(kv) d(kv)$$

Results and Discussion

This thesis investigates the generation of spectral hole burning and its precise control using the effective phase of driving fields in a Doppler-broadened medium. Spectral hole burning refers to the selective bleaching of absorption in a medium at specific frequencies due to molecular distribution. In this study, the atomic decay rate is set to 1 GHz, with other frequencies scaled relative to this rate. The Doppler width (VDV_DVD) is assumed to be 10710^7107, while parameters ω\omega$\omega$, k0=2π/λk_0 = 2\pi / \lambda$k0=2π/λ, and ω=c·k0\omega = c \cdot k_0$ω=c·k0 are employed, where k0k_0k0 represents the free-space wave-vector of electromagnetic waves.

Figure 4.1 illustrates the real and imaginary parts of the electric susceptibility (χ\chi$\chi$) under Doppler broadening. The imaginary component corresponds to the absorption spectrum of the probe beam, while the real part relates to the dispersion spectrum. Normal dispersion occurs when the refractive index (nrn_rnr) increases with frequency (dnr/dω>0dn_r/d\omega > 0$dnr/dω>0), while anomalous dispersion is observed when nrn_rnr decreases with frequency (dnr/dω<0dn_r/d\omega < 0$dnr/dω<0). The refractive index is linked to susceptibility by the relation nr=1+2πRe(χ)n_r = 1 + 2\pi \text{Re}(\chi)nr =1+2πRe(χ).

The spectral holes are analyzed at three phase values: $\phi_c=0$\phi_c = 0$φc=0, $\phi_c=\pi/6$\phi_c = \pi/6$φc=π/6, and $\phi_c=\pi/4$\phi_c = \pi/4$φc=π/4. At $\phi_c = 0$\phi_c = 0$φc=0, two spectral holes are observed in the absorption spectrum at detuning values $\Delta_p=\pm 1.57$\Delta_p = \pm 1.57$Δp=±1.57. The spectral hole at $\Delta_p=+1.57$\Delta_p = +1.57$Δp=+1.57 is larger, with a steeper normal dispersion compared to the hole at $\Delta_p=-1.57$\Delta_p = -1.57$Δp=−1.57. This steep

dispersion leads to a significantly larger group index, dramatically slowing the group velocity (vgv_gvg) of the pulse relative to the speed of light in a vacuum (ccc), as shown in **Figure 4.1a**.

At $\phi c = \pi/6$\phi_c = \pi/6$\phi c=\pi/6$, the depth of the spectral hole at $\Delta p = -1.57$\Delta_p = -1.57$\Delta p=-1.57$ increases, while it decreases at $\Delta p = +1.57$\Delta_p = +1.57$\Delta p=+1.57$. Consequently, the normal dispersion around $\Delta p = -1.57$\Delta_p = -1.57$\Delta p=-1.57$ intensifies, while it gradually reduces near $\Delta p = +1.57$\Delta_p = +1.57$\Delta p=+1.57$, as shown in **Figure 4.1b**.

At $\phi c = \pi/4$\phi_c = \pi/4$\phi c=\pi/4$, the depth of the spectral hole at $\Delta p = -1.57$\Delta_p = -1.57$\Delta p=-1.57$ further increases, while the hole at $\Delta p = +1.57$\Delta_p = +1.57$\Delta p=+1.57$ continues to decrease, indicating a further variation in dispersion characteristics.
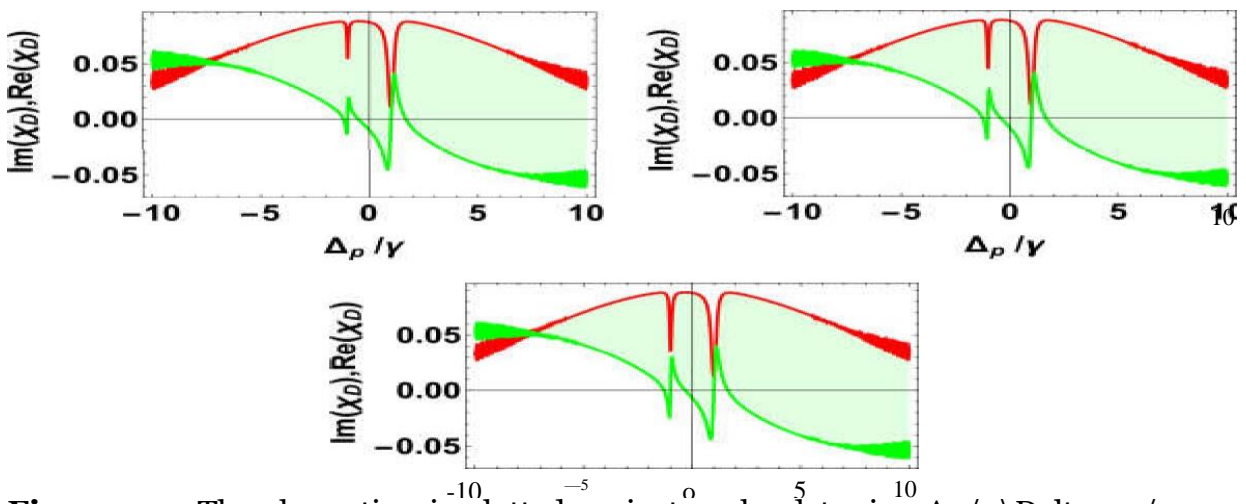
Figure 4.1: The absorption is plotted against probe detuning $\Delta p/\pi$\Delta_p / \pi$\Delta p/\pi$, where values of 0.0270.0270.027, $\Delta I2 = 0.7$\Delta I_2 = 0.7$\Delta I2=0.7$, and G=27G = 27G=27 are considered. In panel (a), when the phase $\phi c = 0$\phi_c = 0$\phi c=0$, the absorption spectrum shows spectral holes at detuning values of $\Delta p = \pm 1.57$\Delta_p = \pm 1.57$\Delta p=\pm1.57$. At phase $\phi c = 0$\phi_c = 0$\phi c=0$, the spectral hole at $\Delta p = +1.57$\Delta_p = +1.57$\Delta p=+1.57$ is larger, and the hole at $\Delta p = -1.57$\Delta_p = -1.57$\Delta p=-1.57$ is smaller. In panel (b), the normal dispersion in the region of $\Delta p = -1.57$\Delta_p = -1.57$\Delta p=-1.57$ is enhanced, while the dispersion at $\Delta p = +1.57$\Delta_p = +1.57$\Delta p=+1.57$ is gradually degraded. In panel (c), the dispersion at $\Delta p = -1.57$\Delta_p = -1.57$\Delta p=-1.57$ continues to improve, and the dispersion at $\Delta p = +1.57$\Delta_p = +1.57$\Delta p=+1.57$ further degrades.

Figure 4.2: The real and imaginary parts of electric susceptibility (χ\chi$\chi$) are plotted in the presence of Doppler broadening for three different phases: $\phi c = \pi/2$\phi_c = \pi/2$\phi c=\pi/2$ and $\phi c = 2\pi/3$\phi_c = 2\pi/3$\phi c=2\pi/3$. Two spectral holes are again observed in the absorption spectrum at detuning values of $\Delta p = \pm 1.57$\Delta_p = \pm 1.57$\Delta p=\pm1.57$ for phase $\phi c = \pi/3$\phi_c = \pi/3$\phi c =\pi/3$. As in the previous case, the spectral hole at $\Delta p = +1.57$\Delta_p = +1.57$\Delta p =+1.57$ is larger, while the hole at $\Delta p = -1.57$\Delta_p = -1.57$\Delta p=-1.57$ is smaller. The slope of the dispersion in the spectral hole regions shows steep normal dispersion, with the dispersion at $\Delta p = +1.57$\Delta_p = +1.57$\Delta p=+1.57$ being more normal compared to the dispersion at $\Delta p = -1.57$\Delta_p = -1.57$\Delta p=-1.57$.

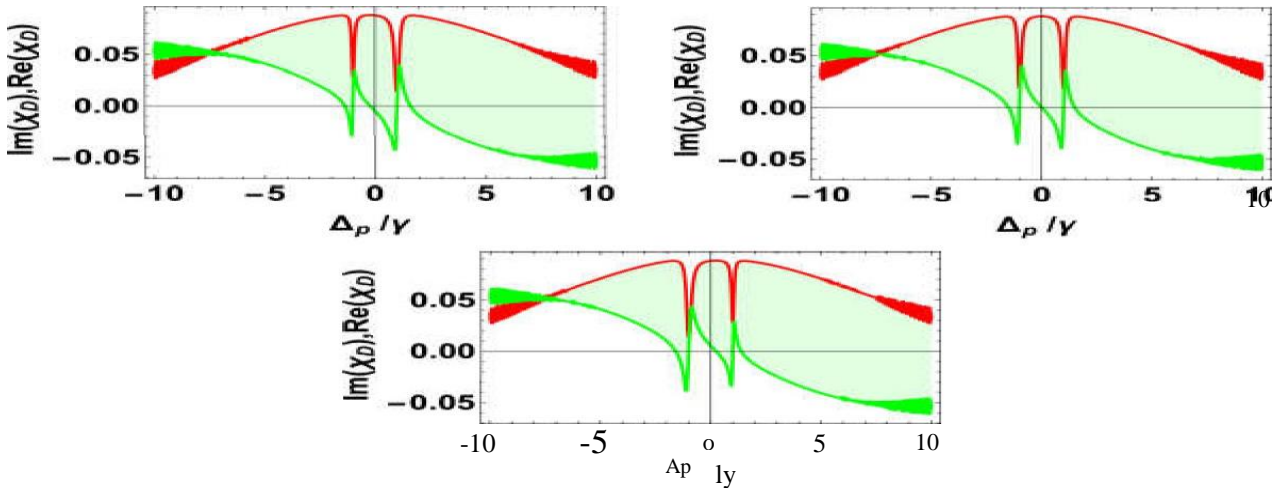The normal dispersion causes the group index to behave accordingly.

Figure 4.2: The absorption is plotted against probe detuning Δ_p/π\Delta_p / \pi$\Delta_p/\pi$, with parameters 0.0270.0270.027, $\Delta I2=0.7$\Delta I_2 = 0.7$\Delta I2=0.7$, and G=27G = 27G=27. Panel (a) shows the phase $\phi c=\pi/3$\phi_c = \pi/3$\phi c=\pi/3$, where the pulse's group velocity significantly slows down due to a large group index, as shown in **Figure 4.2a**. At phase $\phi c=\pi/2$\phi_c = \pi/2$\phi c=\pi/2$ (panel b), the depths of both spectral holes at $\Delta p=\pm 1.57$\Delta_p = \pm 1.57$\Delta p=\pm 1.57$ are equal, resulting in identical steep normal dispersion at both detuning regions. Finally, at phase $\phi c=2\pi/3$\phi_c = 2\pi/3$\phi c=2\pi/3$ (panel c), the depth of the spectral hole at $\Delta p=-1.57$\Delta_p = -1.57$\Delta p=-1.57$ increases, while the depth at $\Delta p=+1.57$\Delta_p = +1.57$\Delta p=+1.57$ decreases. This leads to a larger normal dispersion at $\Delta p=-1.57$\Delta_p = -1.57$\Delta p=-1.57$ and a smaller dispersion at $\Delta p=+1.57$\Delta_p = +1.57$\Delta p=+1.57$.

Figure 4.3: The real and imaginary parts of electric susceptibility (χ\chi$\chi$) are plotted in the presence of Doppler broadening. Spectral holes are analyzed at three different phases: $\phi c=3\pi/4$\phi_c = 3\pi/4$\phi c=3\pi/4$, $\phi c=5\pi/6$\phi_c = 5\pi/6$\phi c=5\pi/6$, and $\phi c=\pi$\phi_c = \pi$\phi c=\pi$. Two spectral holes are observed at detuning values $\Delta p=\pm 1.57$\Delta_p = \pm 1.57$\Delta p=\pm 1.57$ at phase $\phi c=\pi/3$\phi_c = \pi/3$\phi c=\pi/3$, with the spectral hole at $\Delta p=+1.57$\Delta_p = +1.57$\Delta p=+1.57$ being smaller and the hole at $\Delta p=-1.57$\Delta_p = -1.57$\Delta p=-1.57$ being larger. The normal dispersion at $\Delta p=+1.57$\Delta_p = +1.57$\Delta p=+1.57$ is less steep compared to that at $\Delta p=-1.57$\Delta_p = -1.57$\Delta p=-1.57$. At phase $\phi c=3\pi/4$\phi_c = 3\pi/4$\phi c=3\pi/4$ (panel a), the depth of the spectral hole at $\Delta p=-1.57$\Delta_p = -1.57$\Delta p=-1.57$ increases while the hole at $\Delta p=+1.57$\Delta_p = +1.57$\Delta p=+1.57$ becomes smaller. The normal dispersion is stronger at $\Delta p=-1.57$\Delta_p = -1.57$\Delta p=-1.57$ and weaker at $\Delta p=+1.57$\Delta_p = +1.57$\Delta p=+1.57$. In panel (b) at phase $\phi c=5\pi/6$\phi_c = 5\pi/6$\phi c=5\pi/6$, the depth of the hole at $\Delta p=-1.57$\Delta_p = -1.57$\Delta p=-1.57$ increases further, and the hole at $\Delta p=+1.57$\Delta_p = +1.57$\Delta p=+1.57$ shrinks even more. The dispersion at $\Delta p=-1.57$\Delta_p = -1.57$\Delta p=-1.57$ becomes larger, while at $\Delta p=+1.57$\Delta_p = +1.57$\Delta p=+1.57$, it becomes smaller. At phase $\phi c=\pi$\phi_c = \pi$\phi c=\pi$ (panel c), the depth of the spectral hole at $\Delta p=-1.57$\Delta_p = -1.57$\Delta p=-1.57$ reaches its maximum, and the hole at $\Delta p=+1.57$\Delta_p = +1.57$\Delta p

Vol. 2 No. 4 (November) (2024)

=+1.57 is most degraded. The normal dispersion profile at $\Delta p=-1.57$\Delta_p = -1.57$\Delta p=-1.57$ is enhanced compared to that at $\Delta p=+1.57$\Delta_p = +1.57Δp =+1.57.
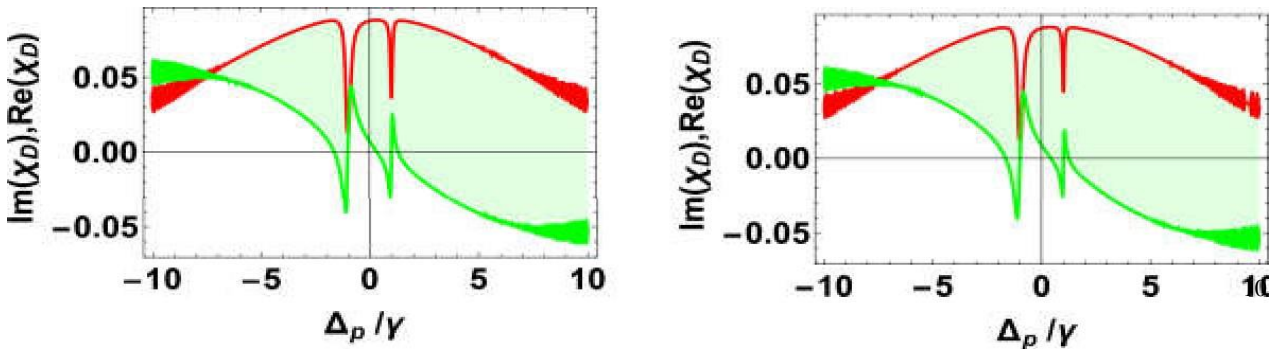
Figure 4.3: Absorption is plotted against probe detuning $\Delta P/\pi$\Delta P / \pi \Delta P/\pi$, where

0.0270.0270.027, $\Delta I2=0.7$\Delta I_2 = 0.7\Delta I2=0.7$, and $G=27$G = 27$G=27$.

Conclusion:

In conclusion, this study investigates the generation of spectral hole burning and its effective control via the phase of the driving fields in a Doppler-broadened four-level sodium atomic medium. Two spectral holes are measured in the absorption spectrum at detunings of $\Delta P=\pm1.57$\Delta P = \pm 1.57\Delta P=\pm1.57$. The steep normal dispersive region within the spectral hole burning zone is also explored. The group velocity is observed to slow down significantly in this normal dispersive region, with the pulse velocity vgv_gvg much smaller than the vacuum speed ccc. At phase $\phi c=\pi/2$\phi_c = \pi/2$\phi c=\pi/2$, the depths and normal dispersion on both sides of the resonance point are equal. However, for phases $\phi c<\pi/2$\phi_c < \pi/2$\phi c<\pi/2$, the depths and normal dispersions are unequal, with a smaller spectral hole at negative detuning and a larger hole at positive detuning. When $\phi c>\pi/2$\phi_c > \pi/2$\phi c>\pi/2$, the trend reverses, with a larger spectral hole at negative detuning and a smaller one at positive detuning. These results highlight the tunability of spectral holes through phase variation and demonstrate the corresponding enhancement and degradation of normal dispersion profiles within the spectral hole regions. This work contributes to the understanding of spectral hole burning and its potential optical applications, such as in optical tomography and photosynthesis.

References

Wei, X. G., WII, J. H., Wang, H. H., Li, A., Kang, Z. H., Jiang, Y., & Gao, J. Y. (2006). First-principles experimental observation of coherent hole burnings in atomic rubidium vapor. *Phys. Rev. A*, 063820.

Vries, H. D., & Wiersma, D. A. (1976). Homogeneous broadening of optical transitions in organic mixed crystals. *Phys. Rev. Lett.*, 36(91).

Muller, A., Richter, W., & Kador, L. (1998). Persistent spectral hole burning in the few-molecule limit: terrylene in p-terphenyl. *Phys. Lett.*, 285(92).

Chaneliere, T., Bonarota, M., Damon, V., et al. (2010). Light storage protocols in Tm:YAG. *J. Lumin.*, 130, 1572.

Colice, M., Schlottau, F., & Wagner, K. H. (2006). Broadband radio-frequency spectrum analysis in spectral-hole-burning media. *Appl. Optics*, 45, 6393.

Mattias, N., Lars, R., Stefan, K., Robert, K., & Dieter, S. (2004). Hole-burning techniques for isolation and study of individual hyperfine transitions in inhomogeneously broadened solids demonstrated in Pr3+:Y2SiO5. *Phys. Rev. B*, 70, 214116.

Li, Y., Hemmer, P., Kim, C., Zhang, H., & Wang, L. V. (2008). Detection of ultrasound-modulated diffuse photons using spectral-hole burning. *Optics Express*, 16, 14862.

Robin, P., & Silvia, V. (2009). Spectral hole burning: examples from photosynthesis. *Photosynth. Res.*, 101, 245.

Harris, T. L., Sun, Y., Babbitt, W. R., et al. (2000). Spatial-spectral holographic correlator at 1536 nm using 30-symbol quadriphase- and binary-phase-shift keyed codes. *Opt. Lett.*, 25, 85.

Schwartz, S. E., & Tan, T. Y. (1967). Wave interactions in saturable absorbers. *Appl. Phys. Lett.*, 10, 4.

Gorokhovskii, A. A., Kaarli, R. K., & Rebane, L. A. (1974). Hole burning in the counter of a pure electronic line in a Shol'skii system. *JEPT Lett.*, 20, 216.

Kharlamov, B. M., Personov, R. I., & Bykovskaya, L. A. (1974). Stable 'gap' in absorption of solid solutions of organic molecules by laser irradiation. *Opt. Commun.*, 12, 191.

Shakhmuratov, R. N., & Szabo, A. (1998). Phase-noise influence on coherent transients and hole burning. *Phys. Rev. A*, 58, 3099.

Dong, P., & Gao, J. Y. (2000). Appearance and disappearance of hole-burning behind an electromagnetically induced transparency window. *Phys. Lett. A*, 265, 52.

Xiao, Z. H., WII, J. H., Zhang, H. F., & Gao, J. Y. (2003). Comparison of coherent induced hole-burning between A, V and ladder systems. *Phys. Lett. A*, 310, 363.

WII, J. H., Wei, X. J., Wang, D. F., Chen, Y., & Gao, J. Y. (2004). Coherent hole-burning phenomenon in a Doppler-broadened three-level A-type atomic system. *J. Opt. B*, 6, 54.

Camacho, R. M., Pack, M. V., & Howell, J. C. (2006). Slow light with large fractional delays by spectral hole-burning in rubidium vapor. *Phys. Lett. A*, 74, 033801.

Agarwal, G. S., & Dey, T. N. (2003). Slow light in Doppler-broadened two-level systems. *Phys. Rev. A*, 68, 063816.

Kuang, S., Du, P., Wan, R., Jiang, Y., & Gao, J. (2008). Slow light based on coherent hole-burning in a Doppler-broadened three-level A-type atomic system. *Optics Express*, 16, 11604.

Abd-Elnabi, S. (2014). Coherent hole burnings induced without saturation field in a Doppler-broadened four-level N-type atomic system. *Optik*, 125, 1620.

Vol. 2 No. 4 (November) (2024)

Kash, M. M., & Sautenkov, V. A. (1999). Ultraslow group velocity and enhanced nonlinear optical effects in a coherently driven hot atomic gas. *Phys. Rev. Lett.*, 82, 5229.

Kasapi, A., Jain, M., Yin, G. Y., & Harris, S. E. (1995). Electromagnetically induced transparency: propagation dynamics. *Phys. Rev. Lett.*, 74, 2447.

Rebane, L. A., Gorokhovskii, A. A., & Kikas, J. V. (1982). Low-temperature spectroscopy of organic molecules in solids by photochemical hole burning. *Appl. Phys. B*, 29, 235.

Meixner, A. J., Renn, A., & Wild, U. P. (1989). Electromagnetically induced transparency: propagation dynamics. *J. Chem. Phys.*, 91, 6728.

Wei, X. G., WII, J. H., Wang, H. H., Kang, Z. H., Jiang, Y., & Gao, J. Y. (2006). First-principles experimental observation of coherent hole burnings in atomic rubidium vapor. *Phys. Rev. A*, 74, 063820.

Fujita, K., Tanaka, K., Hirao, K., & Soga, N. (1998). Room-temperature persistent spectral hole burning of Eu3+ in sodium aluminosilicate glasses. *Opt. Lett.*, 23, 543.